An Acad Bras Cienc (2023) 95(Suppl. 3): e20210816 DOI 10.1590/0001-3765202320210816
Anais da Academia Brasileira de Ciências | *Annals of the Brazilian Academy of Sciences*
Printed ISSN 0001-3765 I Online ISSN 1678-2690
www.scielo.br/aabc | www.fb.com/aabcjournal

PHYSICAL SCIENCES

Aerosol optical properties over the South Atlantic and southern ocean during the 2010-2012 summer seasons as part of the global maritime aerosol network

PAULA S. PEREIRA, ELAINE A. DOS SANTOS, HEITOR EVANGELISTA, NEWTON MAGALHAES & ALEXANDER SMIRNOV

Abstract: Aerosols have implications to climate and biogeochemical cycles in the global oceans. At sites under indirect influence of dust emitted by the Patagonian semi-desert, a debate exists on the potential fertilization effects of iron enriched aerossol. Considering this subject we conducted measurements of aerosols optical properties using a Microtops II sun photometer to access aerosol size distributions and other intrinsic properties oversea from Atlantic Southern mid-latitudes to Antarctica. Oceanographic cruises were developed between December 2010 to April 2011 and October 2011 to April 2012, in the context of the Brazilian Antarctic Program, and between November 2011 to December 2011. This survey was taken as part of the Global Maritime Aerosol Network (MAN/NASA). Our data of AOD (500 nm) along the South American coast depicts a steady decrease southwards following the decreased latitudinal continental extent. However, the influence of the aerosols blown from Patagonia semi-desert region was clear from latitude 53ºS to 64ºS. The predominance of aerosol fine mode was observed in Central Atlantic and close to the Drake Passage. An unexpected aerosol coarse mode predominance was found close to the Antarctic Peninsula. We attribute that to a possible weathering of rock outcrops due to the strong westerly winds in that region.

Key words: Aerosols, South Atlantic, AOD, Antarctica, Maritime Aerosol Network.

INTRODUCTION

Aerosols play a role in the climate control through the energy balance by the absorption or scattering of solar radiation. They take part in the formation of clouds and precipitation, influencing the albedo and the atmospheric visibility (Aoki et al. 2006, Redmond et al. 2010). Moreover, their composition, size distribution, and chemical reactions in the atmosphere can contribute to the air heating or cooling influencing biogeochemical cycles in terrestrial and marine environments as a whole (Duce & Tindale 1991, Mahowald et al. 2009, Baker & Croot 2012).

According to Mcmurry (1999) and Kulkarni et al. (2011), aerosols suspended in the atmosphere are two-phase systems, consisting of a solid or a liquid phase, with a surrounding gas phase. They can have lithological, marine, biogenic, anthropic or cosmogenic origins and, according to their formation processes, they can be primary or secondary, that is, reach the atmosphere directly from the source or through chemical reactions, respectively (Claeys et al. 2010, Kulkarni et al. 2011). The oceans are one

of the most important sources of aerosols. The predominant type is the sea salt, found in the aerosol coarse mode. They are emitted from oceans's surface through sea spray and breaking bubbles and waves. A second important type is originated from Dimethyl Sulfide (DMS) degassing derived from blooms of algal biomass. DMS is oxidized in the atmosphere producing, sulfate aerosols that act as condensation nuclei (Seinfeld & Pandis 1998, Wilson 2011). Those from continental origin, such as volcanic ash and semi-desert dust stand out as natural sources. They may reach the oceans, where they participate in biogeochemical cycles related to primary productivity (Martin & Fitzwater 1988, Moore et al. 2013).

Depending on the type, source and interactions in the atmosphere their size may vary between 1 nm to 100 μm. The optical properties of aerosols derive from their interactions with solar radiation of short and long wavelengths, which involve absorption, reflection, and refraction (Shaw et al. 1973). They may be represented by the aerosol optical depth (AOD), Ångström coefficient, albedo scattering, linear extinction coefficient, relative phase function, and refractive indexes (Wilson 2011). AOD measures the extinction of direct solar radiation, at different wavelengths, when it passes through the atmosphere. Estimates of the aerosol size can be achieved optically by the Ångström exponent (α) since it is a parameter that describes the relationship between the optical thickness of an aerosol type and the wavelength of the sunlight. The Ångström exponent is inversely related to the average size of the aerosols (Evangelista et al. 2010, Moore et al. 2013. Particularly over the Argentine Continental Shelf, the Southern Atlantic and corresponding Southern Ocean Sector a debate exists on the potential role of dust storms carrying iron enriched aerosols to the increase of primary productivity (Meskhidze et al. 2007). Iron solubility and bioavailability are crucial to trigger phytoplanktonic blooms and are parameters linked to the chemical composition and size distribution of rosols. Therefore, measuring aerosol optical properties oversea allow characterizing their size distribution and may infer the potential role of aerosols to "ocean fertilization". Additionally, these properties are fundamental to study the relation between aerosols and cloud formation in the marine environment (Smirnov et al. 2011).

The objective of the present research is to survey the aerosol optical properties at the Southwestern Atlantic and corresponding Southern Ocean Sector from *in situ* measurements, using a sun photometer during oceanographic campaigns in 2010, 2011 and 2012, in the context of the Brazilian Antarctic Program and the Global Maritime Aerosol Network under the support of NASA Goddard Space Flight Center (Smirnov et al. 2002).

MATERIALS AND METHODS

Oversea measurements and study region

Optical measurements were taken onboard the Polar Vessel NPo Almirante Maximiano of the Brazilian Navy during the austral spring-to-summer seasons. Two cruises (1A and 1B) covered the coastal region from Rio de Janeiro City, in Brazil, (22.924° S; 43.259° W) to the Northern Antarctic Peninsula (64.102° S; 56.393° W) enclosing the Southwestern Atlantic, the Drake Passage and the South Shetland Islands from December 8, 2010 to April 24, 2011 and from October 8, 2011 to April 28, 2012. A second vessel, Hydro-oceanographic R/V Cruzeiro do Sul, covered a track from Southern Africa (33.903° S; 18.425 °E) to Central South Atlantic (35° S; 26.358° W) between November 7, 2011 to December 14, 2011 (Figure 1).

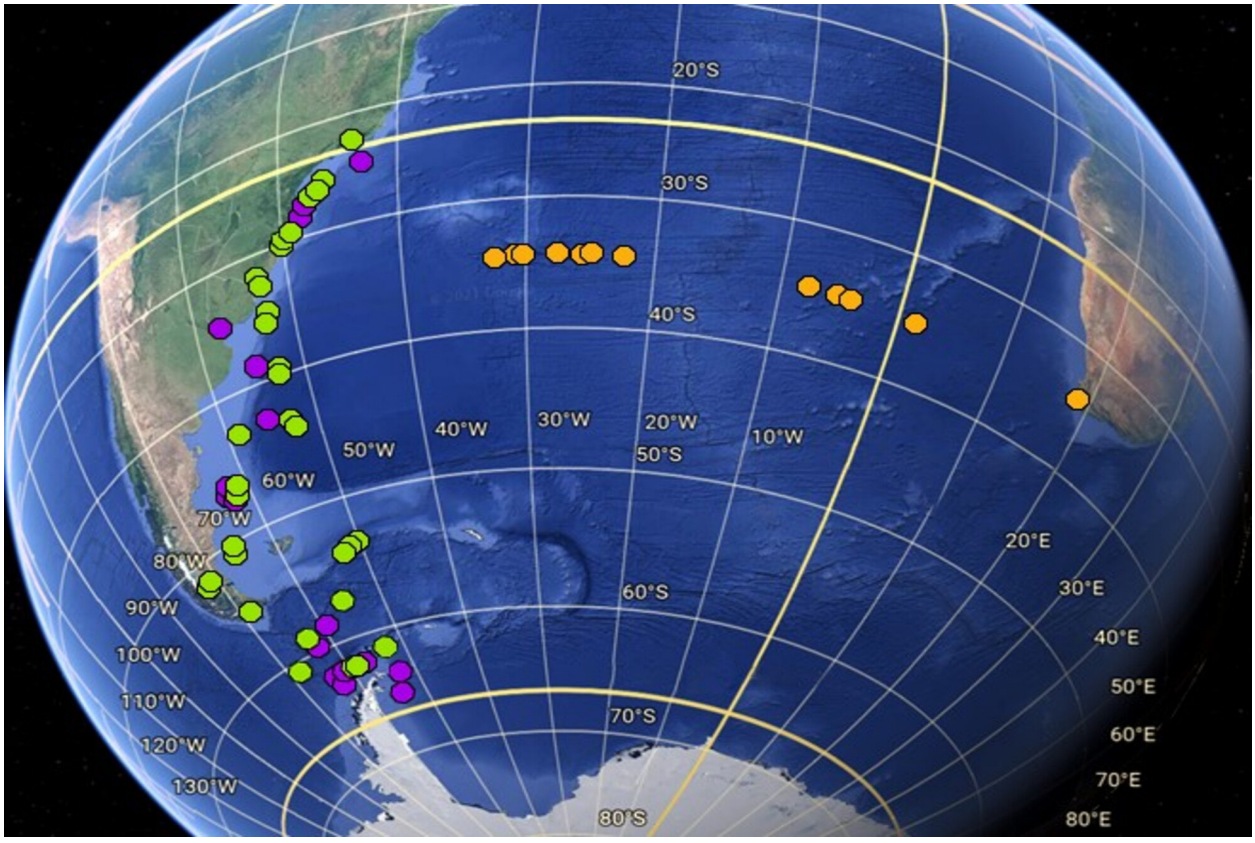

Figure 1. Location of measuring points: Cruise1A: Expedition NPo Almirante Maximiano 2010-2011 (purple); Cruise 1B: Expedition NPo Almirante Maximiano 2011-2012 (green); Cruise 2: NHo Cruzeiro do Sul Expedition 2011 (orange).

Data acquisition

The measurements were performed using the handheld sun photometer Microtops II (Supplementary Material - Figure S1) which database is available from the Maritime Aerosol Network (MAN) website (http://aeronet.gsfc.nasa.gov/new_web/maritime_aerosol_network.html). A component of the AErosol RObotic NETwork (AERONET), from NASA (Wilson et al. 2010, Smirnov et al. 2002). MAN operates oversea during vessel expeditions using a standard manual portable sun photometer (Wilson et al. 2010, Smirnov et al. 2002).

The equipment performs spectral measurements of direct solar radiation attenuation over the ocean and light scattering angular properties, acquiring accurate measurements from aerosol optical properties along atmospheric column through five spectral channels, that can be disposed in different combinations, between the spectral bands from 340 nm to 1020 nm. (Smirnov et al. 2002light absorption coefficient, and single scattering albedo (omega(0).

The sun photometer Microtops II calculates AOD spectral values in the wavelengths 440, 500, 675 e 870, total water vapor in the specific atmospheric column from the bandwidth 940 nm, Zenital angle and α. All data available in MAN has been calibrated by Spectral Deconvolution Algorithm (SDA), which generates three quality levels: level 1.0 (unscreened), level 1.5 (cloud screened) and 2.0 (cloud screened and quality assurance). The third one has high quality control and accuracy, since

its calibration has been tested in various optical conditions and also calculates α, classifying the particle in coarse or fine mode. (Smirnov et al. 2011). In this study, level 2.0 algorithm was applied to the dataset and the bandwidth at 500 nm was chosen as a standard, to help comparisons with past studies, which have the same subject and uses this wavelength. The average of the measurement results are shown in table I.

Measurements were made according to clarity and clear sky conditions, aiming the equipment directly to the sunlight, during daylight when the sun was not obstructed by clouds and when the solar zenith angle not too large. The first cruise (1A) in Southwestern and Austral Oceans had 111 measurements, while the second (1B), 1188. The cruise in Central Atlantic Ocean had 187 measurements (or samples).

Microtops II calculates the direct solar radiation to acquire AOD, α and water vapor, which is defined by the Beer-Lambert-Bouguer law:

$$V(\lambda) = V_0\left(\lambda\right)\left(\frac{d_0}{d}\right)^2 e^{\left(-m\tau_t(\lambda)\right)} \quad (1)$$

where V is the digital voltage of the equipment in each wavelength (λ), representing the solar irradiance; V_0 is the spectral irradiance from exo-atmosphere, $\frac{d_0}{d}$ is the rate between the average d_0 and the actual (at the time of reading) d distance between earth and sun a; m is the solar zenit angle and $\tau_t(\lambda)$ is the total atmospheric optical depth. (Knobelspiesse et al. 2004, Wilson et al. 2010)

When calculate AOD, other atmospheric constituents must be considered. The optical depth due to trace gases, water vapor and Rayleigh scattering must be subtracted from the total optical depth to obtain just the aerosol component:

$$T(\lambda)_{Aerosol} = \tau_t(\lambda) - \tau(\lambda)_{water} - \tau(\lambda)_{Rayleigh} - \tau(\lambda)_{O_3} - \tau(\lambda)_{CO_2} - \tau(\lambda)_{NO_2} - \tau(\lambda)_{CH_4} \quad (2)$$

Ångström Exponent is the first derivate of AOD in logarithmic scale and can be calculated from the wavelengths, typically between 440-870 nm using least squares fit. The first derivate of AOD (Wilson, 2011). Values greater than 1.0 indicate fine mode particles and near zero, indicate coarse mode particles.

$$\alpha = -\left(\frac{d\ln\tau_a}{d\ln\lambda}\right) \quad (3)$$

where α is Ångström exponent; τ_a is AOD and λ, the wavelength.

Water vapor parameter has equal importance to define aerosol optical properties and its influence in global radiation budget and climate change (Ichoku et al. 2002). The water atmospheric column vapor amount determination uses three channels: 675 nm, 870 nm e 940 nm, and the bandwidth between 936 e 940 nm comprises a strong vibrational combination interval f water vapor). absorption (Halthore et al. 1997). The total transmission (T) i calculated for 675 nm e 870 nm using Rayleigh and aerosol optical depths. The total transmission for 940 nm (T_{940}) is defined through extrapolation. The extrapolated transmission at 940 nm is subtracted is subtracted from the measured transmission at 940nm (T_{940}), providing the transmission only due to water vapor (Tw).

$$\ln\left[T_w\right] = \ln\left[T_{940[medido]}\right] - \ln\left[T_{940[extrapolado]}\right] \quad (4)$$

$$-\ln\left[T_w\right] = \ln\left[V_{0\,940} * d^{-2}\right] - \ln\left[V_{940}\right] - m*\left(\tau_{940\ AOT} + \tau_{940\ Rayleigh}\right) \quad (5)$$

$$-\ln[T_w] = a*(m_w*u)^b \quad (6)$$

$$u = \frac{\left[\frac{-\ln T_w}{a}\right]^{1/b}}{m_w} \quad (7)$$

where u is the precipitable water in cm; T_w is the transmission due to water vapor; a e b are filter-dependent constants and m_w is the water vapor optical air mass (Schmid et al. 2001, Smirnov et al. 2003).

Data analyses

K-means classification

The K-means classification technique, as proposed by Wilson et al. (2010) and Knobelspiesse et al. (2004), was used in this study to group the data into two cluster with similar nature, each one, in this case, with AOD (500 nm) and Ångström Exponent daily means values to divide the data into aerossol size: fine and coarse mode. The technique begins by randomly selecting your data, then two centers clusters were chosen to reflect the statistical difference between them through the minimum Euclidean distance. The clustering separation evaluates the quality of the data taken during the expeditions.

Air mass back-trajectory model (HYSPLIT/NOAA)

For a consistent interpretation of the optical data provided by the Microtops II Sun Photometer, HYSPLIT (HYbrid Single-Particle Lagrangian Integrated Trajectory) model was used to run backward trajectories of air mass parcels during the measurements along the cruises. The model aims at tracing the migration history of the aerosols transported in the air mass parcel. It is available for public use at the ARL portal (Air Resources Laboratory) of NOAA (National Oceanic and Atmospheric Administration) and it is a hybrid combination of Lagrangian and Eulerian approaches that calculate the displacement of air masses and particles concentrations changes along their trajectories. The meteorological database used in the modeling was NCEP/ NCAR (National Centers for Environmental Prediction / National Center for Atmospheric Research) Reanalysis Project (Draxler & Hess 1998). In this work, the air masses backward trajectories were run for 120 hours using daily means measurements for each cruise.

RESULTS AND DISCUSSION

It has been observed that the aerosols in the study region are diverse in nature and highly influenced by westerly winds derived of marine, semi-deserts, and volcanic origins (Martin & Fitzwater 1988).

Figure 2 depicts latitudinal and longitudinal values of AOD and Ångström coefficient throughout the sampling period in the three transects. They show a predominance of the coarse fraction along the coast, over the Atlantic Ocean and Antarctica, with some exceptions of fine fractions nearby the coast. Highest AOD values were found in lower latitudes and lowest values in Central South Atlantic and Southern South America Oceans.

The interpretation of the database in Figure 2 was based on previous studies presented as a compilation in Table I.

Table I. Standard values for aerossol classification by interested geographic locations.

Region	Type of environment	AOD	α	References
General Classification	Clean environment Marine Desert Continental	0.01 <0.15 0.2-0.4 0.2	- <1.0-coarse mode 0-0.5- coarse mode 1.0-1.5	Porter et al. 2000 Smirnov et al. 2003, Knobelspiesse et al. 2004, Toledano et al., 2007
Coast of Africa	Coastal/marine	0.03-0.12	Fine and coarse mode	Wilson et al. 2010
South Atlantic Ocean	Marine Desert Continental	<0.1 0.18 0.16	0.0-0.4-coarse mode 0.20 0.89	Knobelspiesse et al. 2004, Smirnov et al. 2006, Sakerin et al. 2007.
Antarctica	Coastal areas Open ocean	0.01-0.06	0.5-1.2-coarse mode and fine 0.7+-0.2-coarse mode	Tomasi et al. 2007, Wilson et al. 2010, Chaubey et al. 2011.

Database from Cruise 1A

Regarding the Cruise 1, that refers to Southwestern Atlantic and the corresponding sector of Southern Ocean, AOD values ranged from 0.02 to 0.28 during campaign 1A and between 0.02 to 0.26 in 1B, while Ångström coefficient ranged from 0.14 to 2 -10 in 1A and -0.02 to 1.5 in 1B, with the highest values of both parameters closer to continental borders, as expected. In the Latitudes 20°S and 30°S there was the highest α values, while between 45°S and 55°S, the lower AOD. The latitudinal gradient of AOD, differently from the expected trend based on previous studies (Smirnov et al. 2003, Sakerin et al. 2007, Wilson et al. 2010), that is, a steady decrease towards higher latitudes, presented a surprising increase between latitudes of 55°S and 65°S (Figure 2a). Figure 2b depicts a two-group aerosol classification as fine and coarse modes. According to Knobelspiesse et al. (2004) the group classification in a scatter plot supports the inference on aerosol type, where low values of AOD with α below 1.0 refer to aerosols predominantly from marine origins, high AOD and α values less than 1.0 to dust, and high AOD values with α greater than 1.0 to continental aerosols (Smirnov et al. 2003). The above classification was performed on basis in the K-means cluster algorithm as proposed by Knobelspiesse et al. (2004) and Wilson et al. (2010)–as showed in figure 2b. The limit (0.5) of both modes different than expected (1.0). The histogram in Figure 2f-indicates that the highest frequency of α values was between 0.4 and 0.8 and, therefore, represent coarse mode, possibly related to sea salt influence and dust blown from the nearby continent. Latitudinal AOD means in different wavelengths and α means (Figures 2c, 2d and 2e) demonstrated a decreasing trend in general, except for α means in the first cruise (1A) that can be explained because of less measurements comparing to cruise 1B.

Concerning the water vapor content in both cruises it was observed a similar trend with values between ~ 0.40 - 4.46 (Figure S2) similar to the studies by Sakerin et al. (2007) and Wilson et al. (2010). These data are corroborated with the decadal variability of the satellital specific humidity (Figure S2b), processed from the NCEP/NCAR Reanalysis Project.

The general database allowed distinguish two geographic zones in this research: Southwestern South Atlantic coast and Antarctic Peninsula. A greater aerosol amount in atmospheric column was observed in Southwestern South Atlantic between latitudes of 20°S and 35°S. According to figure

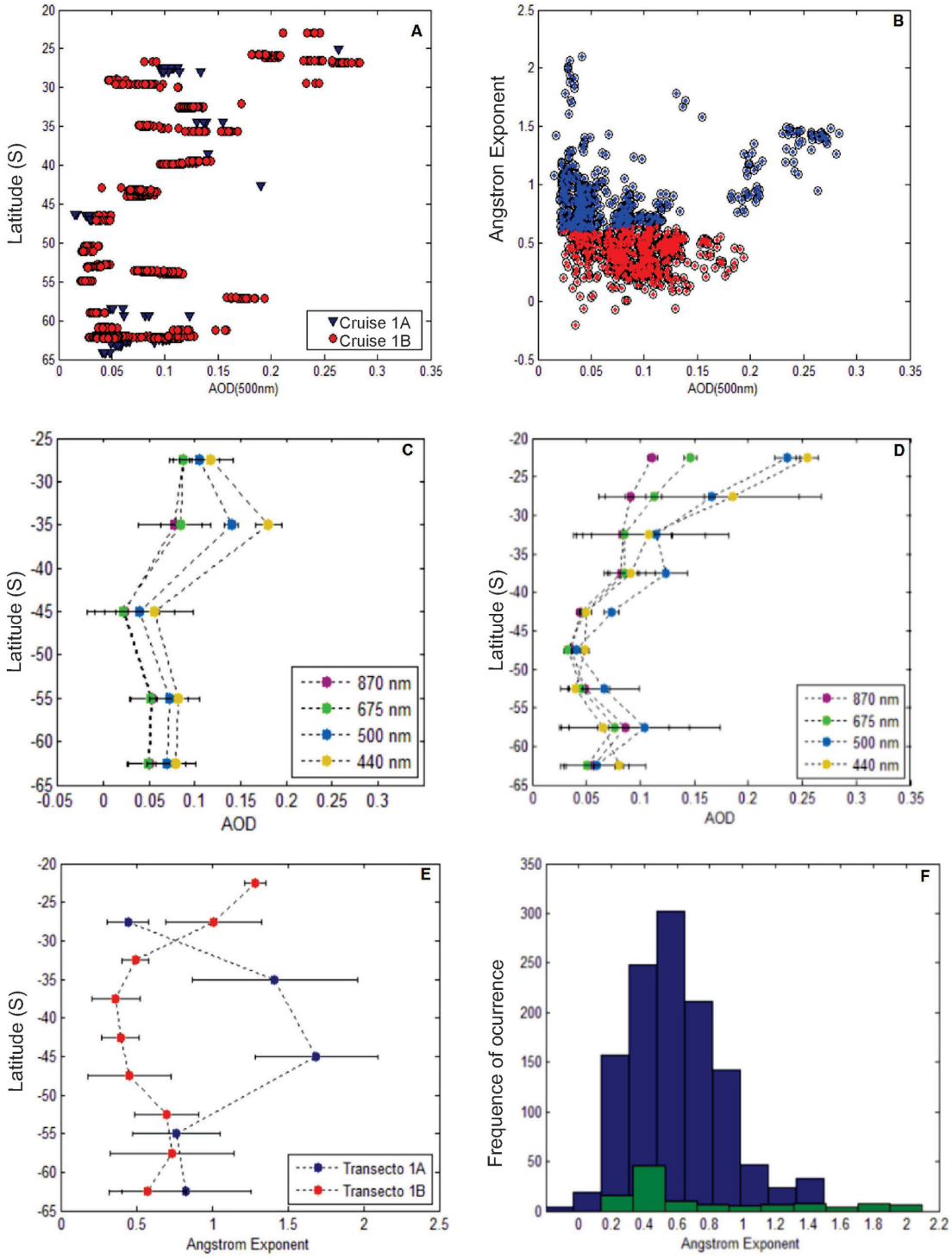

Figure 2. (a) Distribution of AOD data in the study area; (b) the same for the Angstrom coeficiente. Basic database for Cruises 1A and 1B. (a) Latitudinal distribution of AOD (500 nm); (b) K-means cluster analysis of AOD data (500 nm) with respect to AE Angstrom coefficient identifying two groups: blue (fine mode) and red (coarse mode); (c) latitudinal averages of AOD at different wavelengths (cruise 1A); (d) latitudinal averages for AOD at different wavelengths (cruise 1B); (e) latitudinal mean values for AE; (f) F: AE frequency distribution: in green: cruise 1A and in blue: cruise 1B.

3, aerosols on Southwestern South Atlantic are concentrated in two main groups, the first one with high AOD and α greater than 1.0, indicating fine mode, are possibly aerosols from continental origins and the second group comprising aerosols with lower AOD, classified as both fine and coarse mode, with a predominance of coarse one. These are possibly from marine origins, such as sea salt, dust from Patagonian semi-desert or a mixture of them. The aerosols along Antarctic Peninsula presented a diverse distribution of both AOD and α with predominantly low AOD values and high α (Figure 3b). According to Wilson et al. 2010, low values of AOD and fine mode dominance are expected to occur in remote sites due to the large distance from aerosol sources and the presence of sea ice, that suppresses the formation of the coarse mode sea salt aerosol. Chaubey et al. (2011) associates high values of α and low AOD in Antarctic Peninsula to the occurrence of strong winds on the ocean surface that generate large sea salt particles. Also, for the same region Mishra et al. (2015) observed a dominance coarse mode of aerossol in autumn-to-winter seasons, while during summer and spring the Aitken and the accumulation modes are dominant in addition to the formation of condensation nuclei (Hara et al. 2011). In this study, AOD values observed in this region were considered high for this type of environment (close to 0.15).

Backward Trajectories Analysis for Cruise 1A and 1B

Backward trajectories were modeled corresponding to all days of measurements. Most important ones are presented in Figure 4. For Cruises 1A and 1B, at SE Brazil air mass trajectories were clearly influenced by an extra-tropical cyclonic system that moves the air parcels counterclockwise bringing marine influence to the continent (Figure S3a). AOD values were ~0.24 with indicating fine mode

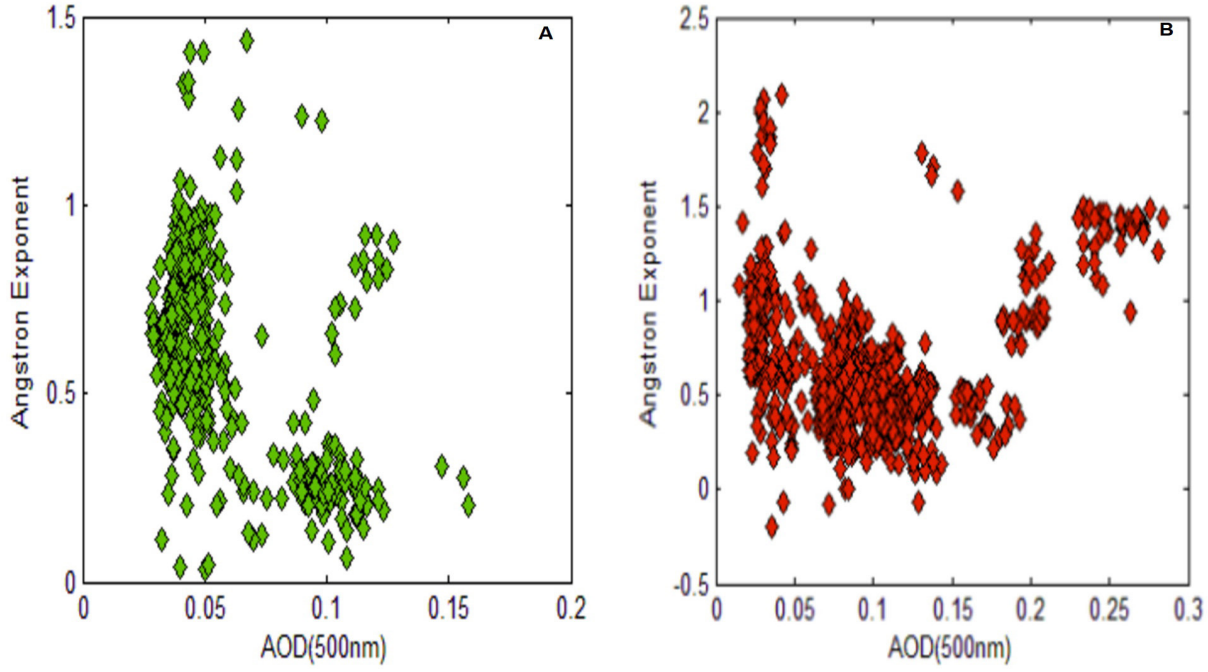

Figure 3. AOD versus AE for Cruises to transects 1A and 1B. (a) relation AOD and Angstrom Exponent for Southwestern Atlantic; (b) AOD and Angstrom Exponent for Antarctic Peninsula.

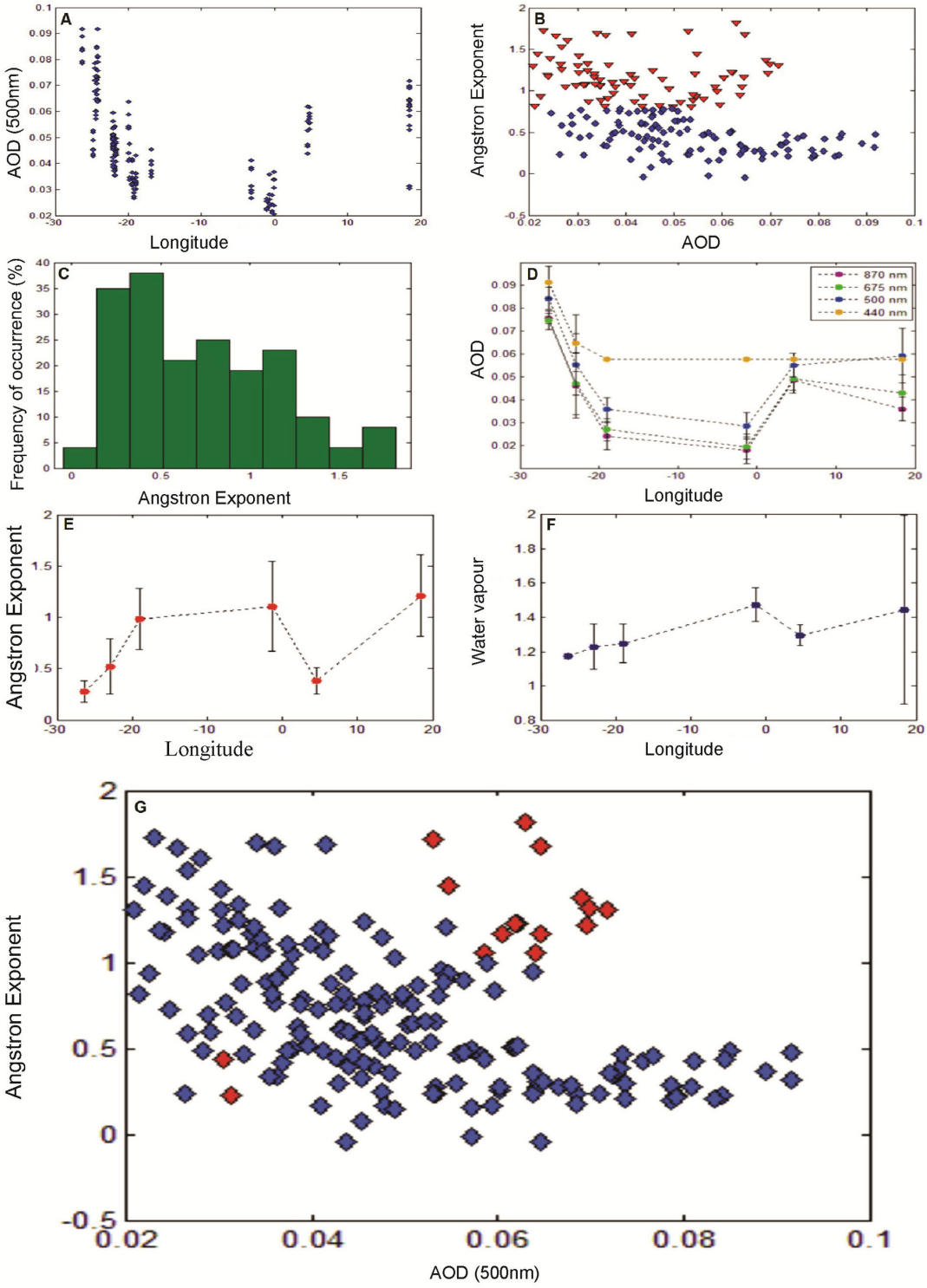

Figure 4. Basic database for Cruise 2. a: longitudinal distribution of AOD (500 nm); b: K-means cluster analysis of AOD data (500 nm) and AE identifying two groups: blue (coarse mode) and red (fine mode); c: Histogram of AE; d: Distribution of longitudinal AOD averages at different wavelengths; e: Distribution of longitudinal averages of water vapor; f: Distribution of longitudinal means of AE; G: Distribution of AOD and AE: red (costal region of Africa) and blue (ocean region).

dominance, which can be related to-continental influence over polluted areas of Rio de Janeiro and São Paulo cities. In contrast, Figure S3b shows a rapid advection from the Patagonia semi-desert mixed with marine influence along the migrating passway. At this point, the AOD values were 0.09 and α less than 1.0, suggesting coarse mode aerossol presence. Close to of 30°S, the backward trajectories show air masses advecting predominantly from Atlantic Ocean (Figure S3c) corresponding to the observed coarse mode. In Figure S3d at La Plata basin, was observed a continental contribution to the aerosol amount corresponding to fine mode with an AOD of 0.15. In sampling station shown in Figure S3e, a mixture of marine and Patagonian influence was observed with coarse aerossol mode dominance. Around latitude 50°S, Figure S3f, were observed fine and coarse aerosol modes corresponding to ir mass migrations starting in the Pacific Ocean and, crossing the Southern Patagonia. In this are AOD was 0.18 suggesting a predominance of continental dust.

The results for Southwestern Atlantic continental border depicted a scenario of rapid aerosol changes interleaving influences of Patagonia semi-desert and nearby ocean.

For the sampling sites corresponding to the surrounding of Northern Antarctic Peninsula, air mass backward trajectory analysis showed a major influence of Antarctic continent and Southern Ocean with one episode of northern advection (Figure S4a). In that case both fine and coarse modes were observed which would correspond to continental and marine mixed sources. In Figure S4b, where a high marine influence is present, mostly derived from Southern Pacific sector, coarse mode was predominant. It was interesting observe that although trajectories at Figures S4d and S4d were relatively similar (derived from the Antarctic Peninsula), a predominant fine mode corresponded to Figure 4c and a coarse mode to Figure 4d. This can be attributed due to different wind intensities occurring during each measurement. In Figure S4e, air mass trajectories indicate contributions from Weddell sea and Southern Atlantic Ocean (Figure S4f). Despite none apparent continental influence, during measurements, fine mode was present together with coarse mode, which can be derived from marine influence. The fine mode presence in the subpolar environment can not be explained solely by the parametrizations presented in this study and may be a more complex process which involves particles interactions and biogeochemical mechanisms linked to the ocean primary productivity. According to Wilson (2011), coarse mode aerosols in Antarctica refers to sea salt and ice crystals in the lower atmosphere while the fine ones to biological activity mainly with sulfates production, as well as nitrate and organic compounds. Another potential source of fine mode can be attributed to ice-free regions like nunataks and proglacial ice free areas that are enhanced during the summer season. Similar to the results observed by Santos et al. (2020) with aerosol provenance studies they occur at several sites of the Maritime Antarctica (example: at South Shetland Islands, James Ross and Peter islands, Dry Valleys, Adelie Land, Bunger Hills, Fyfe Hills and Mawson Coast) and its dust can be mixed in the lower atmosphere by westerly winds actions.

Chaubey et al. (2011) observed a coarse mode predominance during winter season, while, in this study, it was observed from different campaigns that coarse mode can also prevail during the summer/spring/autumn seasons.

Database from Cruise 2

Cruise 2 refers to the transect from Central- South Atlantic to Atlantic coast of Southern Africa. Along the cruise AOD values ranged from 0.02 to 0.09 (Figure 4a). This result indicates predominantly, an

clean environment. Ångström Exponent values ranged between -0.04 and 1.82, which higher values were mostly located close to African continent where AOD ranges from ~ 0.03 to 0.07, similarly to Wilson (2011) which values were between ~ 0.04 and 0.09. Otherwise, in this region, α values were 1.8, differently from Wilson (2011) that observed 1.1. AOD values are enhanced at coastal regions and decrease nearly exponentially towards Central South Atlantic where the lower AOD values were found, as showed in Figure 4a with all data and Figure 4d, in different wavelengths. Figure 4b shows a consistent aerosol classification into two groups by using K-means cluster algorithm, similarly to Figure 5B. In this case, the limit between both groups was 1.0. The histogram for α in Figure 4c indicates that modal classes ranges from 0.2 to 0.5 and therefore, are mostly related to coarse mode aerosols, possibly attributed to sea salt. Longitudinal means (Figures 4c and 4f) showed similar trends, demonstrating low α values, that is, coarse mode aerosols and high water vapor values in oceanic areas, as well as, high α (fine mode aerosols) and low water vapor values nearby coastal regions. Figure 4g corroborates this, classifying the data into two geographic groups.

Backward Trajectories Analysis for Cruise 2

Likewise cruises 1A and 1B, backward trajectories were modeled to corresponding sampling points during campaign 2. In offshore region, air masses migrations were influenced by westerlies and the South Atlantic gyre. The long track developed by air masses over sea resulted in a predominance of coarse mode, with greater AOD as the case of Figure S5a. In longitudes at Central South Atlantic, fine mode was predominant, where low AOD values were observed (Figure S5b and S5c). Fine aerosols mode was found closer to the African continent as shown in Figure S5e and S5f.

Figure 5 and table II summarizes total database and shows how fine and coarse mode, based on AOD, were spatially distributed (colors purple and green refer to coarse mode, and yellow and orange fine mode). It can be observed that fine mode prevailed at sub-tropical latitudes while course mode at Central South Atlantic, Southern Argentine Continental Shelf and Antarctica. Fine modes found in Central South Atlantic and Antarctica may be related to long distance advection of fine dust from adjacent continents or by aerosols from biogenic origin.

Table II. Summary of aerosol properties mean values for the total dataset. SD: standard deviation.

Locations	AOD 500nm	SD_{500}	α	SDα	Water vapor (cm)	STDwy	AOD 440nm	SD_{440}	AOD 675nm	SD_{675}	AOD 870nm	SD_{870}
South America Coast	0,10	0,08	0,76	0,33	1,74	0,93	0,11	0,08	0,08	0,05	0,07	0,04
South Atlantic (Offshore)	0,09	0,03	0,51	0,21	0,80	0,29	0,07	0,02	0,06	0,02	0,06	0,02
Antarctic (Coast)	0,06	0,03	0,06	0,26	0,62	0,15	0,08	0,03	0,05	0,03	0,06	0,03
South Africa (Coast)	0,05	0,02	0,68	0,40	1,28	0,15	0,06	0,01	0,04	0,02	0,04	0,02
Central Atlantic (Offshore)	0,06	0,01	1,21	0,41	1,45	0,57	0,06	0,00	0,04	0,01	0,04	0,01

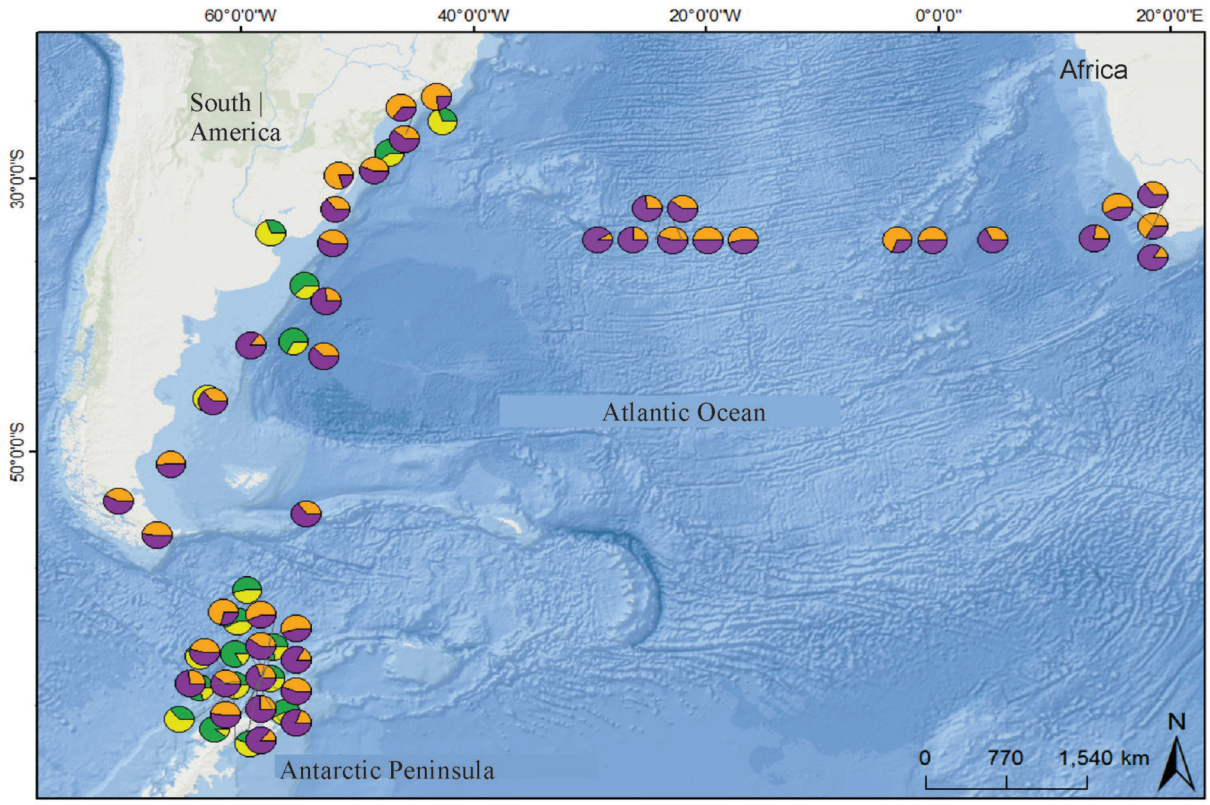

Figure 5. Fine and coarse aerosol modes derived from AOD. The colors purple and green refer to coarse mode, and yellow and orange to fine mode.

CONCLUSIONS

In situ optical measurements from portable Sun Photometer provided insights on aerosol size distribution from mid-to-subpolar latitudes along coastal region of the Southwestern Atlantic and the corresponding Southern Ocean sector and the region between the Central Atlantic and Southern Africa. While compared to airmass backward trajectories, it revealed a high influence of dust advecting from Patagonia semi-desert.

Along the South American coast a steady decrease of AOD (500 nm) was observed following the continental mainland extent. However the influence of the aerosols blown from Patagonia semi-desert region was clear from latitude 53S to 64S. The predominance of aerosol fine mode was concentrated to the Central Atlantic region and close to the Drake Passage. Aerosol coarse mode predominance was found close to the Antarctic Peninsula that could be related to weathering of rock outcrops due to the typical strong westerly winds in that region.

ACKNOWLEDGMENTS

We grateful thank Roberta Priori for graphic layouts and the Brazilian Antarctic Program for logistics during oceanographic cruises.

REFERENCES

AOKI T, MOTOYOSHI H, KODAMA Y, YASUNARI T, SUGIURA K & KOBAYASHI H. 2006. Atmospheric aerosol deposition snow surfaces and its effect on albedo. SOLA 20: 13-16.

BAKER AR & CROOT PL. 2012. Atmospheric and Marine Controls on Aerosol Iron Solubility in Seawater. Mar Chem 120: 1-4.

CHAUBEY JP, MOORTHY KK, BABU SS & NAIR VS. 2011. The optical and physical properties of atmospheric aerosols over the Indian Antarctic stations during southern hemispheric summer of the International Polar Year 2007–2008. Ann Geophys 29: 109-121.

CLAEYS M ET AL. 2010. Chemical characterisation of marine aerosol at Amsterdam Island during the austral summer of 2006-2007. J. Aerosol Sci 41: 13-22.

DUCE RA & TINDALE NW. 1991. Ocean Limnol. Oceanogr 36(8): 715-726.

DRAXLER R & HESS GD. 1998. An overview of the HYSPLIT 4 modelling system for trajectories, dispersion and deposition. Aust Meteorol Mag 47: 295-308.

EVANGELISTA H ET AL. 2010. Inferring episodic atmospheric iron fluxes in the Western South Atlantic. Atmos Environ 44(5): 703-712.

HARA K ET AL. 2011. Seasonal variations and vertical features of aerosol particles in the Antarctic troposphere. Atmos Chem Phys 11: 5471-5484.

HALTHORE RN ET AL. 1997. Sun photometric measurements of atmospheric water vapor column abundance in the 940-nm band. J Geophys Res 102: 4343-4352.

ICHOKU C ET AL. 2002. Analysis of the performance characteristics of the five-channel Microtops II Sun photometer for measuring aerosol optical thickness and precipitable water vapor. J Geophys Res (107): D13-5.

KNOBELSPIESSE KD, PIETRAS C, FARGION GS, WANG M, FROUIN R, MILLER MA, SUBRAMANIAM A & BALCHI WM. 2004. Maritime aerosol optical thickness measured by handheld sun photometers. Remote Sens Environ 93 (1-2): 87-106.

KULKARNI P, PAUL AB & KLAUS W. 2011. Aerosol Measurement: Principles, Techniques, and Applications. 3rd ed., New York: John Wiley & Sons, 904 p.

MAHOWALD N ET AL. 2009. Atmospheric Iron Deposition: Global Distribution, Variability, and Human Perturbations. Annu Rev Mar Sci 1: 245-278.

MARTIN JH & FITZWATER SE. 1988. Iron deficiency limits phytoplankton growth in the north-east Pacific subarctic. Nature 331: 341-343.

MCMURRY PH. 1999. A review of atmospheric aerosol measurements. Atmos Environ 34: 1959-1999.

MESKHIDZE N, NENES A, CHAMEIDES WL, LUO CHAO & MAHOWALD N. 2007. Atlantic Southern Ocean productivity: Fertilization from above or below? Global Biogeochem Cycles 21: GB2006.

MISHRA AK, KOREN I & RUDICH Y. 2015. Effect of aerosol vertical distribution on aerosol-radiation interaction: A theoretical prospect. Heliyon (1): e00036.

MOORE CM, MILLS MM, ARRIGO KR, BERMAN-FRANK I, BOPP L, BOYD PW, GALBRAITH ED, GEIDER RJ, GUIEU C & JACCARD SL. 2013. Processes and patterns of oceanic nutrient limitation. Nat Geosci 6: 701-710.

PORTER JN, MILLER M, PIETRAS C & MOTELL C. 2000. Ship-based sun photometer measurements using sun photometers. J Atmos Ocean Technol 18: 765-774.

REDMOND HE, DIAL KD & THOMPSON J E. 2010. Light scattering and absorption by wind blown dust: theory, measurement, and recent data. Aeolian Res 2: 5-26.

SAKERIN SM, SMIRNOV A, KABANOV DM, POL'KIN VV, PANCHENKO MV, HOLBEN BN & KOPELEVICH OV. 2007. Aerosol optical and microphysical properties over the Atlantic Ocean during the 19th cruise of the Research Vessel Akademik Sergey. J Geophys Res 112 (D10220): 1-9.

SANTOS EA, EVANGELISTA H, VALERIANO CM, NETO CCAN, CASTAGNA A & HEILBROM M. 2020. Origin and radiogenic isotope fingerprinting of aerosols over the Southwestern Atlantic and corresponding Southern Ocean Sector. Aeol Resear 45: 100596.

SCHMID B ET AL. 2001. Comparison of Columnar Water-Vapor Measurements from Solar Transmittance Methods. Appl Optics 40: 1886-1896.

SEINFELD JH & PANDIS SN. 1998. Atmospheric Chemistry and Physics from air pollution to climate change. 1st ed., New York: John Wiley & Sons, 1232 p.

SHAW G, REAGAN JA & HERMANC BM. 1973. Investigations of Atmospheric Extinction Using Direct Solar Radiation Measurements Made with a Multiple Wavelength Radiometer. Amer Meteor Soc 12: 374-380.

SMIRNOV A, HOLBEN BN, ECK TF, DUBOVIK O & SLUTSKER I. 2003. Effect of wind speed on columnar aerosol optical properties at Midway Island. J Geophys Res 108(D24): 4802.

SMIRNOV A, HOLBEN BN, KAUFMAN YJ, DUBOVIK O, ECK TF, SLUTSKER I, PIETRAS C & HALTHORE RN. 2002. Optical properties of atmospheric aerosol in maritime environments. J Atmos Sci 59(3): 501-523.

SMIRNOV A ET AL. 2006. Ship-based aerosol optical depth measurements in the Atlantic Ocean: comparison with satellite retrievals and GOCART model. Geophy Res Lett 33(L14817): 1-4.

SMIRNOV A ET AL. 2011. Maritime aerosol network as a component of AERONET - First results and comparison with global aerosol models and satellite retrievals. Atmos Meas Tech 4(3): 583-597.

TOLEDANO C ET AL. 2007. Aerosol optical depth and Angstr ˚ om exponent climatology at ¨ El Arenosillo AERONET site (Huelva, Spain). Q J R Meteorol Soc 133: 795-807.

TOMASI C ET AL. 2007. Aerosols in polar regions: A historical overview based on optical depth and in situ observations. J Geophys Res Atmos 112: D16205.

WILSON D. 2011. Aerosol optical properties in the South Atlantic Ocean. 2011. 96 f. Dissertation (Master of Science), School of Geography, Archaeology and Environmental Studies, University of the Witwatersrand. (Unpublished).

WILSON DI. ET AL.2010. Aerosol optical properties over the South Atlantic and Southern Ocean during the 140th cruise of the M/VS.A. Agulhas. Atmos Res 98(2-4): 285-296.

How to cite

PEREIRA PS, SANTOS EA, EVANGELISTA H, MAGALHAES N & SMIRNOV A. 2023. Aerosol optical properties over the South Atlantic and southern ocean during the 2010-2012 summer seasons as part of the global maritime aerosol network. An Acad Bras Cienc 95: e20210816. DOI 10.1590/0001-3765202320210816.

Manuscript received on May 29, 2021;
accepted for publication on April 17, 2022

PAULA S. PEREIRA[1]
https://orcid.org/0000-0003-4836-3866

ELAINE A. DOS SANTOS[1]
https://orcid.org/0000-0001-9620-9498

HEITOR EVANGELISTA[1]
https://orcid.org/0000-0001-9832-1141

NEWTON MAGALHAES[1,2]
https://orcid.org/0000-0003-0294-9319

ALEXANDER SMIRNOV[3,4]
https://orcid.org/0000-0002-8208-1304

[1]Universidade do Estado do Rio de Janeiro, Laboratório de Radioecologia e Mudanças Globais/LARAMG, Pavilhão Haroldo Lisboa da Cunha, Subsolo, Rua São Francisco Xavier, 524, Maracanã, 20550-013 Rio de Janeiro, RJ, Brazil

[2]Rio de Janeiro State University (UERJ), Laboratório de Modelagem Geográfica, Department of Physical Geography, Pavilhão João Lyra Filho, R. São Francisco Xavier, 524, Maracanã, 20550-013 Rio de Janeiro, RJ, Brazil

[3]NASA Goddard Space Flight Center (GSFC), Greenbelt, MD 20771, USA

[4]Science Systems and Applications, Inc., 10210 Greenbelt Rd # 600, Lanham, MD 20706, USA

Correspondence to: **Elaine Alves dos Santos**
E-mail: elainealves1301@gmail.com

Author contributions

PSP: Developed the theory and performed the computations. contributed to the writing of the paper. EAS: Compiled atmospheric models and contributed to the interpretation of the results. Performed measurements during oceanographic cruises and contributed to the writing of the paper. HE: Conceived of the research concept Supervised the findings of this work. NM: Performed measurements during oceanographic cruises. AS: Allowed instrumentation for measurements and compilation of data. All authors provided critical feedback and helped shape the research, analysis and manuscript.